Stereoselective Formation of Seven-Coordinate Titanium(IV) Monomer and Dimer Complexes of Ethylenebis(*o*-hydroxyphenyl)glycine

Maolin Guo, Hongzhe Sun, Shailja Bihari, John A. Parkinson, Robert O. Gould, Simon Parsons, and Peter J. Sadler*

Department of Chemistry, University of Edinburgh, King's Buildings, West Mains Road, Edinburgh EH9 3JJ, U.K.

Received June 10, 1999

Reactions between the antitumor agent titanocene dichloride (Cp_2TiCl_2) and the hexadentate ligand *N*,*N*′-ethylenebis(*o*-hydroxyphenylglycine) (H_4ehpg) have been investigated in aqueous solution and the solid state. The racemic ligands give crystals of the monomer **[**Ti(ehpg)(H_2O)**]**·(11/3)H_2O **(1),** while the *meso* ligand gives the oxo-bridged dimer [{Ti(Hehpg)(H_2O)}$_2$O]·13H_2O **(2)**. Complex **1** crystallizes in the monoclinic space group *C*2/*c* with a = 24.149(4) Å, b = 14.143(3) Å, c = 19.487(3) Å, β = 105.371(13)°, V = 6417.7(19) Å^3, Z = 12, and *R(F)* = 0.0499 for 4428 independent reflections having $I > 2\sigma(I)$, and contains seven-coordinate pentagonal-bipyramidal Ti^{IV} with two axial phenolate ligands (Ti−O, 1.869(2) Å). The pentagonal plane contains the two N-atoms at 2.210(2) Å, two carboxylate O-atoms at 2.061(2) Å, and a water molecule (Ti−OH_2, 2.091(3) Å). Complex **2** crystallizes as an oxygen-bridged dimer in the triclinic space group *P*-1 with a = 12.521(6) Å, b = 14.085(7) Å, c = 16.635(8) Å, α = 80.93(2)°, β = 69.23(2)°, γ = 64.33(2)°, V = 2472(2) Å^3, Z = 4, and *R(F)* = 0.0580 for 5956 independent reflections having $I > 2\sigma(I)$. Each seven-coordinate, pentagonal-bipyramidal Ti^{IV} has a bridging oxide and a phenolate as axial ligands. The pentagonal plane donors are H_2O, two carboxylate O-atoms, and two NH groups, which form H-bonds to O-atoms both in the same half-molecule (O···N, 2.93−3.13 Å) and in the other half-molecule (O···N, 2.73−2.75 Å); the second phenoxyl group of each Hehpg ligand is protonated and not coordinated to Ti^{IV}, but H-bonds to a nearby amine proton (O···N, 2.73−2.75 Å) from the same ligand and to a nearby H_2O (O···O, 2.68 Å). In contrast to all previously reported crystalline metal−EHPG complexes containing racemic ligands, in which the N(*S*,*S*)C(*R*,*R*) or N(*R*,*R*)C(*S*,*S*) form is present, complex **1** unexpectedly contains the N(*S*,*S*)C(*S*,*S*) and N(*R*,*R*)C(*R*,*R*) forms. This is attributed to the presence of ring strain in seven-coordinate Ti^{IV} complexes. Moreover, the *rac* ligands selectively form crystals of monomeric **1**, while the *meso* ligand selectively forms crystals of the dimer **2** (N(*R*,*R*)C(*R*,*S*) or N(*S*,*S*)C(*S*,*R*)). Complexes **1** and **2** exhibit phenolate-to-Ti^{IV} charge-transfer bands near 387 nm, and 2D NMR studies indicate that the structures of **1** and **2** in solution are similar to those in the solid state. Complex **1** is stable over the pH range 1.0−7.0, while **2** is stable only between pH 2.5 and pH 5.5. Cp_2TiCl_2 reacts with EHPG at pH* 7.0 to give complex **1** with a $t_{1/2}$ of ca. 50 min (298 K), but complex **2** was not formed at this pH* value. At pH* 3.7, the reaction is very slow: **1** forms with a half-life of ca. 2.5 d, and **2** after ca. 1 week at ambient temperature. The relevance of these data to the possible role of serum transferrin as a mediator for the delivery of Ti^{IV} to tumor cells is discussed.

Introduction

Biscyclopentadienyl−Ti^{IV} complexes and bis(β-diketonato)−Ti^{IV} complexes have been shown to exhibit low toxicity and high antitumor activities against a wide range of murine and human tumors.[1−3] Two of them, titanocene dichloride (Cp_2TiCl_2) and Budotitane [Ti(bzac)$_2$(OEt)$_2$] (Hbzac = 1-phenylbutane-1,3-dionato), are currently on clinical trial. The initial results with Cp_2TiCl_2 suggest a lack of cross-reactivity with cisplatin and patterns of antitumour activity different from those produced by platinum-based anticancer drugs.[4] Recent reports[5] have shown that Cp_2TiCl_2 significantly overcomes cisplatin resistance in ovarian carcinoma cell lines. The potent antitumor activity and low toxicity of this compound, supported by the encouraging results from two recent phase I clinical trials[6] (one in Germany, one in the U.K.), suggest that titanocene dichloride could be a promising novel chemotherapeutic agent.[5] In addition, titanocene dichloride exhibits pronounced antiviral, antiinflammatory, and insecticidal activities.[7] Additional medical interest in titanium

* To whom correspondence should be addressed. Fax: +44 131 650 6452. E-mail: p.j.sadler@ed.ac.uk.

(1) (a) Köpf-Maier, P.; Köpf, H. *Chem. Rev.* **1987**, *87*, 1137−1153 and references therein. (b) Köpf-Maier, P.; Köpf, H. *Drugs Future* **1986**, *11*, 297−319 and references therein. (c) Köpf-Maier, P.; Köpf, H. In *Metal compounds in Cancer Therapy;* Fricker, S. P., Ed.; Chapman & Hall: London, 1994; pp 109−146.

(2) Keppler, B. K.; Friesen, C.; Vongerichten, H.; Vogel, E. In *Metal Complexes in Cancer Chemotherapy;* Keppler, B. K., Ed.; VCH: Weinheim, 1993; pp 297−323.

(3) Sadler, P. J. *Adv. Inorg. Chem.* **1991**, *36*, 1−48.

(4) (a) Berdel, W. E.; Schmoll, H. J.; Scheulen, M. E.; Korfel, A.; Knoche, M. F.; Harstrci, A.; Bach, F.; Baumgart, J.; Sass, G. *J. Cancer Clin. Oncol.* **1994**, *120S*, R172. (b) Köpf-Maier, P. *Eur. J. Clin. Pharmacol.* **1994**, *47*, 1−14. (c) Moebus, V. J., Stein, R.; Kieback, D. G.; Runnebaum, I. B.; Sass, G.; Kreienberg, R. *Anticancer Res.* **1997**, *17*, 815−821.

(5) Christodoulou, C. V.; Eliopoulos, A. G.; Young, L. S.; Hodgkins, L.; Ferry, D. R.; Kerr, D. J. *Br. J. Cancer* **1998**, *77*, 2088−2097.

(6) (a) Kortel, A.; Schmol, H. J.; Scheulen M. E.; Gründel. O.; Harstrick. A.; Knoche. M.; Fels, L. M.; Bach, F.; Baugmart, J.; Sass, G.; Thiel, E.; Berdel, W. E. *ASCO* **1996**, *356*, 38. (b) Christodoulou, C. V.; Ferry, D. R.; Fyfe, D. W.; Young, A.; Doran, J.; Sheehan, T. M. T.; Eliopoulos, A. G.; Hale, K.; Baumgart, J.; Sass, G.; Kerr, D. J. *J. Clin. Oncol.* **1998**, *16*, 2761−2769.

10.1021/ic990669a CCC: $19.00
Published on Web 12/29/1999

arises from the recent use of ^{45}Ti in radiopharmaceuticals.[8] However, in contrast to platinum-based anticancer drugs,[9] very little is known about the biological chemistry of titanium compounds. The cytotoxic action of titanium complexes, and their vanadium and molybdenum analogues, may involve mechanisms different from those of cisplatin.[2,10−13] Formation of Ti^{IV}−DNA complexes is thought to be important for the antitumor properties of Cp_2TiCl_2, which inhibits DNA synthesis rather than RNA and protein synthesis, and from which titanium accumulates in nucleic-acid-rich regions of tumor cells after in vivo or in vitro administration.[14−16] However, unlike cisplatin, Cp_2TiCl_2 does not bind to DNA bases strongly at physiological pH, but forms strong complexes with nucleotides only at low pH.[17] Also, there is no evidence for stable complexes of the V or Mo analogues with nucleotides or DNA under physiological conditions.[10a,13c] This raises doubts about DNA as the predominant target.[10a,13c] Efforts to identify the biologically active Ti species have been largely unsuccessful due to the rapid hydrolysis of the titanium(IV) complexes at neutral pH, which results in precipitation of uncharacterized polymeric hydrolysis products.[2,11a]

Transferrin is an 80 kDa iron-transport protein present in the serum of vertebrates at a concentration of about 35 μM.[18] It carries iron(III) in blood at pH 7.4, delivers it to cells via receptor-mediated endocytosis, and releases it at pH ca. 5−5.5 in endosomes.[18,19] In human serum, only 30% of the transferrin sites are saturated with iron. Many other metal ions have been reported to bind reversibly to human serum transferrin.[18] Moreover, transferrin has been implicated in transport and delivery of therapeutic metal ions such as $^{67}Ga^{III}$ and Ru^{III} to cancer cells.[20,21] Since we have recently found that Ti^{IV} forms a strong complex with human serum transferrin (hTF) by binding to the specific Fe^{III} binding sites,[22] we have now studied in detail the binding of Ti^{IV} to the phenolic ligand ethylenebis(*o*-hydroxyphenylglycine) (EHPG). This ligand itself contains donor groups similar to those of transferrin (2Tyr, His, Asp, and CO_3^{2-}) and has long been used to model metal−transferrin binding. Metal−EHPG complexes have been shown to model not only many of the physical properties of metal−transferrin complexes but also a number of other iron−phenolate proteins.[23−34] In addition, EHPG has been suggested as a potential radiopharmaceutical carrier for positron emission tomography.[33] We have studied the interaction of EHPG with titanocene dichloride and titanium(IV) citrate in aqueous solution over a wide range of pH values, and here report the NMR studies and X-ray crystal structures of two novel Ti−EHPG complexes. The structures reveal a unique stereoselective recognition of the EHPG ligands by Ti^{IV}.

Chart 1. Schematic Drawing of *N*,*N*′-Ethylenebis[(*o*-hydroxyphenyl)glycine] (H_4ehpg)[a]

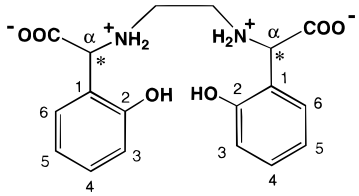

H_4ehpg

[a] The asterisks indicate the chiral α-carbons. The labeling scheme indicated is used for protons in NMR spectra. For complex **2**, a dash is used to label atoms on the uncoordinated phenol (H3′, H4′, etc.)

Experimental Section

Materials. The ligand H_4ehpg (see Chart 1) was purchased from Sigma Chemical Co. and purified as described previously.[26] No attempt was made to separate the racemic *R*,*R*/*S*,*S* and mesomeric *R*,*S* isomers of the ligand, which are present in an unspecified mixture in commercial preparations (subsequently determined to be ca. 1:1 in our samples). Cp_2TiCl_2 was purchased from the Arcos Chemical Co., and monosodium citrate from the Aldrich Chemical Co. Titanium(IV) citrate was prepared as described previously.[22] All other chemicals were AR grade and were used as received.

NMR Spectroscopy. ^1H (500 or 600 MHz) NMR spectra were recorded in D_2O on a Bruker DMX 500 or Varian 600 NMR

(7) Köpf-Maier, P.; Köpf, H. *Struct. Bonding* **1988**, *70*, 105−185.
(8) Ishiwata, K.; Ido, T.; Monma, M.; Murakami, H.; Fukuda, M.; Kammeyama, K.; Yamada, K.; Endo, S.; Yoshioka, S.; Sato, T.; Matsuzawa, T. *Appl. Radiat. Isot.* **1991**, *42*, 707−712.
(9) (a) Sudquist, W. I.; Lippard, S. J. *Coord. Chem. Rev.* **1990**, *100*, 293−322. (b) Berner-Price, S, J.; Sadler, P. J. *Coord. Chem. Rev.* **1994**, *151*, 1−40. (c) Reedijk, J. *Chem. Commun.* **1996**, 801−806. (d) Guo, Z.; Sadler, P. J.; *Angew. Chem., Int. Ed. Engl.* **1999**, *38*, 4001−4019 and reference therein.
(10) (a) Kuo, L. Y.; Liu, A. H.; Marks, T. J. *Met. Ions Biol. Syst.* **1996**, *33*, 53−85, and references therein. (b) Yang, P.; Guo, M. *Met.-Based Drugs* **1998**, *5*, 41−58. (c) Yang, P.; Guo, M. *Coord. Chem. Rev.* **1999**, *185*−*186*, 189−211 and references therein.
(11) (a) Toney, J. H.; Marks, T. J. *J. Am. Chem. Soc.* **1985**, *107*, 947−953. (b) Murray, J. H.; Harding, M. M. *J. Med. Chem.* **1994**, *37*, 1936. (c) Yang, P.; Guo, M. *Met.-Based Drugs* **1998**, *5*, 146−153. (d) Mokdsi, G.; Harding, M. M. *Met.-Based Drugs* **1998**, 5, 207−215.
(12) Toney, J. H.; Brock, C. P.; Marks, T. J. *J. Am. Chem. Soc.* **1986**, *108*, 7263−7274.
(13) (a) Kuo, L. Y.; Mercouri, G.; Kanatzidis, M. S.; Marks, T. J. *J. Am. Chem. Soc.* **1987**, *109*, 7207. (b) Kuo, L. Y.; Kanatzidis, M. S.; Sabat, M.; Tipton, L.; Marks, T. J. *J. Am. Chem. Soc.* **1991**, *113*, 9027−9045. (c) Harding, M. M.; Mokdsi, G.; Mackay, J. P.; Prodigalidad, M.; Lucas, S. W. *Inorg. Chem.* **1998**, *37*, 2432−2437. (d) McLaughlin, M. L.; Cronan, J. M., Jr.; Schaller, T. R.; Sneller, R. D. *J. Am. Chem. Soc.* **1990**, *112*, 8949−8952.
(14) Köpf-Maier, P.; Köpf, H.; Wagner, W. *Cancer Chemother. Pharmacol.* **1981**, *5*, 237.
(15) Köpf-Maier, P.; Krahl, D. *Chem.-Biol. Interact.* **1983**, *44*, 317−328.
(16) (a) Köpf-Maier, P.; Martin, R. *Virch. Arch. B Cell Pathol.* **1989**, *57*, 213−222. (b) Köpf-Maier, P. *J. Struct. Biol.* **1990**, *105*, 35−45.
(17) Guo, M.; Sadler, P. J. Unpublished results.
(18) (a) Baker, E. N. *Adv. Inorg. Chem.* **1994**, *41*, 389−463. (b) Aisen, P. *Met. Ions Biol. Syst.* **1998**, *35*, 585−631. (c) Sun, H.; Cox, M. C.; Li, H.; Sadler, P. J. *Struct. Bonding* **1997**, *88*, 71−102. (d) Sun, H.; Li, H.; Sadler, P. J. *Chem. Rev.* **1999**, *99*, 2817−2842.
(19) (a) Weaver, J.; Pollack, S. *Biochem. J.* **1989,** *261*, 789−792. (b) Weaver, J.; Zhan, H.; Pollack, S. *Br. J. Haematol.* **1993**, *83*, 138−144.
(20) Chitambar, C. R.; Matthaeus, W. G.; Antholine, W. E.; Graff, K.; O'Brien, W. J. *Blood* **1988**, *72*, 1930.
(21) Kratz, F.; Hartmann, M.; Keppler, B. K.; Messori, L. *J. Biol. Chem.* **1994**, *269*, 2581−2588.
(22) Sun, H.; Li, H.; Weir, R.; Sadler, P. J. *Angew. Chem., Int. Ed. Engl.* **1998**, *37*, 1577−1579.
(23) Gaber, B. P.; Miskowski, V.; Spiro, T. G. *J. Am. Chem. Soc.* **1974**, *96*, 6868.
(24) Ainscough, E. W.; Brodie, A. M.; Plowman, J. E.; Brown, K. L.; Addison, A. W.; Gainsford, A. R. *Inorg. Chem.* **1980**, *19*, 9, 3655.
(25) Harris, W. R.; Carrano, C. J.; Pecoraro, V. L.; Raymond, K. N. *J. Am. Chem. Soc.* **1981**, *103*, 2231.
(26) Pecoraro, V. L.; Harris, W. R.; Carrano, C. J.; Raymond, K. N. *Biochemistry* **1981**, *20*, 7033.
(27) Patch, M. G.; Simolo, K. S.; Carrano, C. J. *Inorg. Chem.* **1982**, *21*, 2972−2977.
(28) Riley, P. E.; Pecoraro, V. L.; Carrano, C. J.; Raymond, K. N. *Inorg. Chem.* **1983**, *22*, 3096−3103
(29) Patch, M. G.; Simolo, K. P.; Carrano, C. J. *Inorg. Chem.* **1983**, *22*, 2630.
(30) Pecoraro, V. L.; Bonadies, J. A.; Marrese, C. A.; Carrano, C. J. *J. Am. Chem. Soc.* **1984**, *106*, 3360.
(31) Carrano, C. J.; Spartalian, K.; Appa Rao, G. V. N.; Pecoraro, V. L.; Sundaralingam, M. V. *J. Am. Chem. Soc.* **1985**, *107*, 1651−1658.
(32) Bonadies, J. A.; Carrano, C. J. *J. Am. Chem. Soc.* **1986**, *108*, 4088−4095.
(33) Bannochie, C. J.; Martell, A. E. *J. Am. Chem. Soc.* **1989**, *111*, 4735−4742.
(34) Lin, W.; Welsh, W. J.; Harris, W. R. *Inorg. Chem.* **1994**, *33*, 884−890.

spectrometer. ^{1}H chemical shifts were referenced to 1,4-dioxane (internal). The 2D COSY, 2D DQFCOSY, and 2D NOESY data were obtained using standard techniques. All spectra were recorded at 298 K unless otherwise stated. The water resonance was suppressed by presaturation or via the WATERGATE pulsed-field-gradient sequence.[35]

pH Measurements. The pH values were determined using a Corning 240 pH meter equipped with an Aldrich micro combination electrode, calibrated with Aldrich buffer solutions at pH 4, 7, and 10. The pH-meter readings for D_2O solutions are recorded as pH* values, i.e., uncorrected for the effects of deuterium on the glass electrode. Adjustments of pH were made with HCl or NaOH (DCl or NaOD for samples in D_2O).

UV−Vis and FT-IR Spectra. UV−vis spectra at different pH values were recorded in 0.1 M NaCl solution on a Shimadzu UV-2501PC spectrophotometer at 298 K, using 1 cm path length cells. Concentrations of complexes **1** and **2** were determined by measuring the Ti content using the ICP-AES technique. The FT-IR spectra were recorded on a Perkin-Elmer Paragon 1000 spectrometer using KBr pellets.

Synthesis of [Ti(ehpg)(H$_2$O)]·(11/3)H$_2$O (1). Cp_2TiCl_2 (124.5 mg, 0.5 mmol) was dissolved in boiling distilled water (10 mL), and H_4-ehpg (180 mg, 0.5 mmol) was added slowly with stirring. The mixture was stirred for 30 min with addition of drops of cold water to keep the volume approximately the same. The resulting deep red-orange solution was filtered while hot to remove traces of unreacted ligand. After cooling to ambient temperature, the pH of the solution was ca. 1.7. One day later, regular rhombic orange crystals were obtained which were suitable for X-ray crystallography. The crystals were filtered and washed 3× with cold water. Yield 73.6% (82.56 mg, based on EHPG-(*rac*), or 36.8% based on Ti). Anal. Calcd for $[Ti(C_{18}H_{16}N_2O_6)(H_2O)]\cdot 5H_2O$, $C_{18}H_{18}N_2O_7Ti\cdot 5H_2O$: C, 42.20; H, 5.50; N, 5.47. Found: C, 42.00; H, 5.32; N, 5.28. FT-IR data (cm^{-1}): 3423br, 1637vs, 1597s, 1478m, 1452m, 1340m, 1250vs, 1188w, 1072w, 1032w, 963w, 901s, 829m, 779m, 761m, 730w, 691w, 646s, 501m, 447w, 428m.

Similar crystals of **1** were also obtainable in lower yield by reaction of titanium(IV) citrate with EHPG (1:1, 20 mM each) in water at 277 K, pH 6.1, for several days.

Synthesis of [{Ti(Hehpg)(H$_2$O)}$_2$O]·13H$_2$O (2). The pH of a solution of 200 mL of titanocene dichloride (249.5 mg, 1.0 mmol) containing 1.0 equiv of H_4ehpg was adjusted to 3.7, and the solution was left at ambient temperature. A week later, large thin orange rectangular plate crystals were obtained, which were suitable for X-ray crystallography. The crystals were fitered and washed 3× with cold water. Yield 47.4% (117 mg, based on EHPG(*meso*), or 23.7% based on Ti). Anal. Calcd for $C_{36}H_{38}N_4O_{15}Ti_2\cdot 9H_2O$: C, 42.21; H, 5.50; N, 5.47. Found: C, 42.53; H, 5.35; N, 5.44. FT-IR data (cm^{-1}): 3422br, 3211br, 1638vs, 1597s, 1480m, 1458m, 1353m, 1294w, 1267m, 1187w, 1106w, 1062w, 1053w, 1006w, 966w, 902w, 790m, 760m, 738m, 702s, 616s, 500m, 434m.

Similar crystals of pure **2** were also obtainable in very low yield from solutions of the same concentration as above at pH 1.9 or at pH 5.0 after about a week at ambient temperature.

X-ray Crystallography. X-ray crystallographic studies of **1** and **2** were carried out on a Stadi-4 diffractometer equipped with an Oxford Cryosystems low-temperature device. Single crystals were mounted at ambient temperature on the ends of quartz fibers in RS3000 oil, and data were collected at 220 K with Mo Kα radiation for **1** and Cu Kα for **2**, using a θ/ω scan mode. ψ-scan data showed no significant intensity variation for **1**, so no absorption correction was applied. The crystal structures were solved by Patterson methods (DIRDIF) (**1**) and by direct methods (SHELXS) (**2**). H-atoms attached to C and N were placed in calculated positions, while those attached to O were located in difference Fourier maps; all were allowed to ride on their parent atoms during subsequent refinement. Both structures were refined by full-matrix least-squares against F^2 (SHELXL). All non-H-atoms were modeled with anisotropic displacement parameters (adps). The final difference map maximum and minimum were +0.75 and −0.38 e Å^{-3} (**1**) and +0.82 and −0.78 e Å^{-3} (**2**). Further crystallographic information is summarized in Table 1.

(35) Piotto, M.; Saudek, V.; and Sklenar, V. *J. Biomol. NMR* **1992**, *2*, 661.

Table 1. Crystal Structure Data for Complexes **1** and **2**

	1	**2**
chemical formula	$[Ti(C_{18}H_{16}N_2O_6)(H_2O)]\cdot(11/3)H_2O$	$[Ti_2O(C_{18}H_{17}N_2O_6)_2(H_2O)_2]\cdot 13H_2O$
fw	488.30	1096.47
color	deep orange	deep orange
cryst syst	monoclinic	triclinic
space group	*C*2/*c*	*P*-1
a (Å)	24.149(4)	12.521(6)
b (Å)	14.143(3)	14.085(7)
c (Å)	19.487(3)	16.635(8)
α (deg)	90	80.93(2)
β (deg)	105.371(13)	69.23(2)
γ (deg)	90	64.33(2)
V (Å^3)	6417.7(19)	2472(2)
Z	12	4
T (K)	220(2)	220(2)
ρ_{calcd} (g·cm^{-3})	1.516	1.473
μ_{calcd} (mm^{-1})	0.462	3.582
F(000)	3056	1152
θ range (deg)	2.56−25.03	2.84−70.01
no. of reflns collected/unique	9463/5662	8694/8070
no. of reflns with $I > 2\sigma(I)$	4428	5956
no. of params	434	729
R1 ($F_0 > 2\sigma(F_o)$)	0.0499	0.0580
wR2 (all data)	0.1340	0.1649

Kinetic Studies of Reactions in Solution. These were carried out at pH* values of 7.0 and 3.7 in D_2O. An aliquot of Cp_2TiCl_2(aq) was introduced into a 5 mm NMR tube charged with EHPG solution (pH* 8.5 or 7.4, respectively) to give a final concentration of 5 mM of each reactant. The pH* values fell to 5.7 or 3.7, respectively, and were readjusted with concentrated NaOD. ^{1}H NMR spectra were recorded immediately, and then subsequently at various time intervals thereafter. There was no measurable change in pH* during the reaction. Similar experiments were performed using titanium(IV) citrate instead of Cp_2TiCl_2. For kinetic analysis of NMR spectra, relative concentrations of each species were calculated at each time point from peak integrals.

Results

Preparations of [Ti(ehpg)(H$_2$O)]·(11/3)H$_2$O (1) and [{Ti(Hehpg)(H$_2$O)}$_2$O]·13H$_2$O (2). The reaction of Cp_2TiCl_2(aq) with commercial EHPG ligand (1 mol equiv) in water afforded orange crystals containing both monomeric [Ti(ehpg)(H$_2$O)] (**1**) and the oxygen-bridged dimer [{Ti(Hehpg)(H$_2$O)}$_2$O] (**2**), containing the *rac* and *meso* isomers of the ligand, respectively (vide infra). The yields of **1** and **2** depended on the pH, the concentrations of the reactants, and the reaction times. Complex **1** has a higher solubility in water (ca. 5 mM) and was stable at low pH (near pH 1), so a good yield of complex **1** was achieved by carrying out the reaction near boiling temperature for 0.5 h at higher concentrations (ca. 50 mM reactants) at pH ca. 1.7. Then crystals formed after the reaction solution was allowed to stand overnight at ambient temperature. The crude crystals obtained under these conditions sometimes contained trace amounts of the dimer **2**, but this was readily removed by washing the crystals with cold water during filtration. Pure crystals of **1** were also obtained from reactions at higher pH (ca. 6.1), using Cp_2TiCl_2 or titanium(IV) citrate as starting material, but the yields were quite low. Complex **2** is stable only over the pH range of ca. 2.5−5.5. It is less soluble (<1 mM) in water at low pH, but dissolves readily at neutral pH, forming a colorless solution. This implies that **2** decomposes at neutral pH. The reaction giving crystals of **2** was quite slow, a good yield being achieved after a week at ambient temperature with low concentrations of reactants (ca. 5 mM) at pH 3.7. Crystals of pure dimer **2** were obtainable without contamination

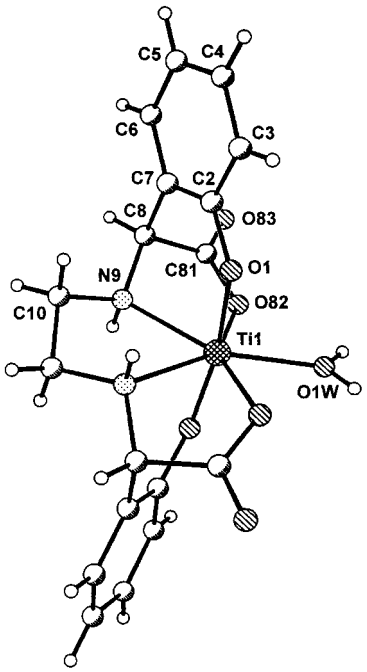

Figure 1. Molecular structure and atom-labeling scheme for one of the mirror isomers of complex **1a**. For complex **1b**, see Figure S1.

by **1**. Pure crystals of **2** were also obtainable at pH ca. 1.9 or 5.0 with the same concentrations of reactants but with very low yields.

X-ray Structure of [Ti(ehpg)(H_2O)]·(11/3)H_2O (1). Two independent molecules (**1a** and **1b**) and their enantiomers (N(*S*,*S*)C(*S*,*S*) and N(*R*,*R*)C(*R*,*R*)) are present in the unit cell. Molecule **1a** lies on a crystallographic 2-fold axis while **1b** is in a general position. They differ slightly in their bond lengths and bond angles (Figure 1, Figure S1 in the Supporting Information, and Table 2). Both contain the racemic isomer of EHPG (*R*,*R* and *S*,*S*). Ti^{IV} exhibits 7-fold coordination with a distorted pentagonal-bipyramidal geometry. In **1a**, the two phenolate oxygen atoms are in the axial positions (O−Ti−O angle, 171.22(14)°; Ti−O, 1.869(2) Å), while the two nitrogen atoms from the two amine groups (Ti−N, 2.210(2) Å), the two oxygen atoms from the two carboxylate groups (Ti−O, 2.061-(2) Å), and an additional oxygen atom from a water molecule (Ti−O, 2.091(3) Å) are nearly equally distributed around the equatorial pentagonal plane of Ti^{IV}. Selected bond lengths and bond angles are given in Table 2. The Ti−N bonds are much longer while the short phenolate Ti−O bond lengths are comparable to those reported previously for Ti^{IV}−phenoxo complexes.[36] The coordinated water molecule is further away, with a bond length similar to those in [Ti^{IV}(EDTA)(H_2O)] (Ti−OH_2, 2.082(2) Å)[37a] and Co^{III}(EDTA)(H_2O)] (Co−OH_2, 2.073-(2) Å).[37b] It forms H-bonds with each of the nearby coordinated carboxylate oxygens (OH···O distance, 2.20 Å). The coordination sphere in **1b** is slightly more distorted than in **1a**, and selected bond lengths and angles are compared in Table 2.

X-ray Structure of [{Ti(Hehpg)(H_2O)}$_2$O)]·13H_2O (2). In the crystal of complex **2**, two molecules, a pair of mirror isomers, appear in the unit cell, and both of them contain only

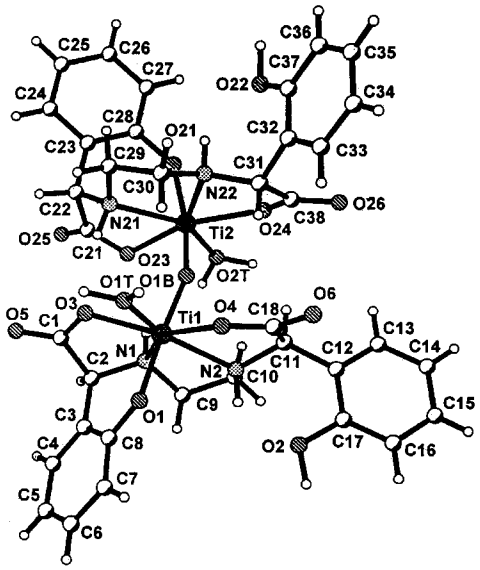

Figure 2. Molecular structure and atom-labeling scheme for one of the mirror isomers of complex **2**.

the *meso* isomer of EHPG. In each of the enantiomers (N(*R*,*R*)C-(*R*,*S*) in both {Ti(Hehpg)(H_2O)} units in one molecule, or N(*S*,*S*)C(*S*,*R*) in both {Ti(Hehpg)(H_2O)} units in the other molecule, one of which is shown in Figure 2), two {Ti(Hehpg)-(H_2O)} units are linked by a μ-O bridge. The Ti^{IV} atoms are also seven-coordinate with a more distorted pentagonal-bipyramidal geometry than that in complex **1**, bound to the bridging oxide, one phenolate group, two nitrogens, two carboxylates, and a water molecule. The other phenol group is protonated and uncoordinated, but forms a hydrogen bond with the nearest amine proton (N···O distance, 2.73−2.75 Å) and a nearby water molecule (O···O distance, 2.68 Å). The coordinated phenolate oxygen and the bridging μ-O atom are located in the axial positions (O−Ti−O angles, 164.6° and 167.4°). The other five coordinated atoms are located in the equatorial plane. The bridging oxygen forms short Ti−O bonds of 1.874(3) and 1.803-(3) Å, and the Ti−O−Ti angle is slightly bent (160.2°). The existence of a nearly linear Ti−O−Ti fragment is also indicated by the strong vibration band[37c] at 702 cm^{-1} in the FT-IR spectrum of **2**. The other bond lengths are comparable to those of **1**. There is extensive hydrogen bonding between the complex and solvent water molecules in the unit cells of both **1** and **2**.

UV−Vis Spectra. The optical spectra of complexes **1** and **2** over the pH range 0.7−8.0 in 0.1 M NaCl are shown in Figure 3. They both exhibit two bands at acidic pH, one below and one above 300 nm. The higher energy band is due to internal ligand transitions, whereas the band centered at 386 nm for **1** and at ca. 388 nm for **2** (the origin of the orange color of the complexes) can be assigned as a ligand-to-metal charge-transfer (LMCT) band. As can be seen from the LMCT bands in Figure 3, complexes **1** and **2** are both more stable at low pH than at high pH. Complex **1** is stable between pH 1.0 and pH 6.5. At pH 7.0, ca. 40% of the absorbance at 386 nm is lost, and by pH > 8.0, the LMCT band has nearly disappeared, corresponding to the loss of Ti^{IV}−phenolate bonding. Complex **2** was less stable than **1**. The LMCT band was observable only between pH 2.5 and pH 6.0. At pH > 7.0, this band disappeared completely. Although the absorbance maximum of the *rac*-EHPG complexes is constant at 386 nm throughout the pH range 1.0−6.4, the absorbance maximum of the *meso*-EHPG complex **2** shifted from 388 nm to a slightly higher wavelength as the

(36) Bird, P. H.; Fraser, A. R.; Lau, C. F. *Inorg. Chem.* **1973**, *12*, 1322−1328.

(37) (a) Fackler, J. P. Jr.; Kristine, F. J.; Mazany, A. M.; Moyer, T. J.; Shephard, R. E. *Inorg. Chem.* **1985**, *24*, 1857−1860. (b) Zubkowski, J. D.; Perry, D. L.; Valente, E. J.; Lott, S. *Inorg. Chem.* **1995**, *34*, 6409−6411. (c) Thewalt, U. and Kebbel, B. *J. Organomet. Chem.* **1978**, *150*, 59−66.

Table 2. Selected Bond Lengths (Å) and Angles (deg) for Complexes **1** and **2** (# = $-x, y, -z + {}^1/_2$)

complex **1a**		complex **1b**			
		Distances (Å)			
Ti(11)−O(11)	1.869(2)	Ti(22)−O(12)	1.866(2)	Ti(22)−O(202)	1.879(2)
Ti(11)−O(821)	2.061(2)	Ti(22)−O(822)	2.056(2)	Ti(22)−O(1332)	2.059(2)
Ti(11)−N(91)	2.210(2)	Ti(22)−N(92)	2.197(3)	Ti(22)−N(122)	2.231(3)
Ti(11)−O(1W1)	2.091(3)	Ti(22)−O(2W2)	2.077(2)		
		Angles (deg)			
O(11)−Ti(11)−O(11#)	171.22(14)	O(12)−Ti(22)−O(202)	168.24(10)		
O(11)−Ti(11)−O(821)	91.64(9)	O(12)−Ti(22)−O(822)	93.18(10)	O(202)−Ti(22)−O(1332)	91.74(10)
O(11)−Ti(11)−O(821#)	90.91(9)	O(12)−Ti(22)−O(1332)	90.51(10)	O(202)−Ti(22)−O(822)	91.41(10)
O(11)−Ti(11)−N(91)	82.74(10)	O(12)−Ti(22)−N(92)	82.22(10)	O(202)−Ti(22)−N(122)	81.60(10)
O(11)−Ti(11)−N(91#)	90.14(10)	O(12)−Ti(22)−N(122)	88.25(10)	O(202)−Ti(22)−N(92)	89.03(10)
O(11)−Ti(11)−O(1W1)	94.39(7)	O(12)−Ti(22)−O(2W2)	95.89(11)	O(202)−Ti(22)−O(2W2)	95.81(11)
O(821)−Ti(11)−O(821#)	146.24(12)	O(822)−Ti(22)−O(1332)	145.92(9)		
O(821)−Ti(11)−N(91)	71.16(8)	O(822)−Ti(22)−N(92)	71.31(9)	O(1332)−Ti(22)−N(122)	70.80(9)
O(821)−Ti(11)−N(91#)	142.47(9)	O(822)−Ti(22)−N(122)	143.13(9)	O(1332)−Ti(22)−N(92)	142.67(10)
O(821)−Ti(11)−O(1W1)	73.12(6)	O(822)−Ti(22)−O(2W2)	72.59(9)	O(1332)−Ti(22)−O(2W2)	73.33(9)
N(91)−Ti(11)−N(91#)	71.91(12)	N(92)−Ti(22)−N(122)	72.41(9)		
N(91)−Ti(11)−O(1W1)	144.05(6)	N(92)−Ti(22)−O(2W2)	143.67(10)	N(122)−Ti(22)−O(2W2)	143.91(9)

Complex **2**			
	Distances (Å)		
Ti(1)−O(1)	1.853(3)	Ti(2)−O(21)	1.944(3)
Ti(1)−O(1B)	1.874(3)	Ti(2)−O(1B)	1.803(3)
Ti(1)−O(4)	2.025(3)	Ti(2)−O(24)	2.045(3)
Ti(1)−O(3)	2.093(3)	Ti(2)−O(23)	2.097(3)
Ti(1)−O(1T)	2.084(3)	Ti(2)−O(2T)	2.095(3)
Ti(1)−N(2)	2.226(3)	Ti(2)−N(22)	2.222(3)
Ti(1)−N(1)	2.241(3)	Ti(2)−N(21)	2.233(3)
	Angles (deg)		
O(1)−Ti(1)−O(3)	91.59(12)	O(21)−Ti(2)−O(23)	87.53(12)
O(1)−Ti(1)−O(4)	99.40(12)	O(21)−Ti(2)−O(24)	91.51(12)
O(1)−Ti(1)−O(1B)	164.59(11)	O(21)−Ti(2)−O(1B)	167.36(11)
O(1)−Ti(1)−O(1T)	93.69(12)	O(21)−Ti(2)−O(2T)	93.77(12)
O(1)−Ti(1)−N(1)	80.70(12)	O(21)−Ti(2)−N(21)	82.73(12)
O(1)−Ti(1)−N(2)	85.73(12)	O(21)−Ti(2)−N(22)	86.20(12)
O(3)−Ti(1)−O(4)	142.98(10)	O(23)−Ti(2)−O(24)	144.09(11)
O(3)−Ti(1)−O(1B)	88.24(12)	O(23)−Ti(2)−O(1B)	91.27(12)
O(3)−Ti(1)−O(1T)	71.65(11)	O(23)−Ti(2)−O(2T)	72.33(11)
O(3)−Ti(1)−N(1)	71.32(11)	O(23)−Ti(2)−N(21)	70.53(11)
O(3)−Ti(1)−N(2)	144.25(11)	O(23)−Ti(2)−N(22)	143.41(12)
O(4)−Ti(1)−O(1B)	90.92(11)	O(24)−Ti(2)−O(1B)	96.79(12)
O(4)−Ti(1)−O(1T)	72.19(11)	O(24)−Ti(2)−O(2T)	71.92(11)
O(4)−Ti(1)−N(1)	145.40(11)	O(24)−Ti(2)−N(21)	144.88(11)
O(4)−Ti(1)−N(2)	72.37(11)	O(24)−Ti(2)−N(22)	72.14(11)
O(1B)−Ti(1)−O(1T)	100.86(11)	O(1B)−Ti(2)−O(2T)	97.85(12)
O(1B)−Ti(1)−N(1)	84.65(12)	O(1B)−Ti(2)−N(21)	85.01(12)
O(1B)−Ti(1)−N(2)	85.43(12)	O(1B)−Ti(2)−N(22)	87.30(12)
O(1T)−Ti(1)−N(1)	142.33(12)	O(2T)−Ti(2)−N(21)	142.81(12)
O(1T)−Ti(1)−N(2)	144.07(12)	O(2T)−Ti(2)−N(22)	144.04(12)
N(1)−Ti(1)−N(2)	73.07(12)	N(21)−Ti(2)−N(22)	72.93(12)
		Ti(1)−O(1B)−Ti(2)	160.22(16)

pH was lowered (401 nm at pH 0.7). This shift implies the formation of protonated metal chelate species.[32]

NMR of Ligands. Commercially available EHPG ligand consists of a mixture of *meso* and *rac* isomers. Since we were able to prepare Ti^{IV} complexes containing either the pure *meso* or *rac* ligand, we have been able to characterize individual isomers of the ligand by NMR. The NMR spectra of free *meso*- or *rac*-EHPG ligands were obtained by acidifying the corresponding Ti^{IV} complex until a colorless solution was obtained. During this process, tiny amounts of white precipitate, presumably polymeric titanium hydroxide, were formed and subsequently filtered off. Since the ^{1}H NMR spectra are in agreement with formation of the free ligand, as can be seen by comparison with the commercial ligand at low pH (Figure S2 in the Supporting Information), no further attempt was made to remove the metal. 1D ^{1}H NMR data on the EHPG isomers at alkaline pH have been published,[27,32] but only the α-protons of the isomers gave distinguishable signals under these analysis conditions. In addition, resonances for the phenyl ring protons of the isomers were unassigned. At pH* values below 2, resonances for all the protons of the isomers of EHPG are well resolved. The ^{1}H NMR spectrum of the commercial ligand is reproduced exactly by combining the spectra of the individual *meso* and *rac* isomers. Unambiguous assignments were established by 2D [^{1}H,^{1}H] COSY and NOESY NMR experiments (Figure S3 in the Supporting Information), and the chemical shifts are listed in Table 3.

NMR of Complexes. Solution-state ^{1}H NMR studies of the diamagnetic Ti^{IV} complexes **1** and **2** allowed comparison of some of their structural features with those in the solid state. Peak assignments were established by 2D NMR techniques. The 2D COSY and 2D NOESY NMR spectra of **1** and **2** in acidic solution are shown in Figures 4 and 5 and Figure S4 in the Supporting Information. The chemical shifts and assignments

Table 3. Comparison of the ^{1}H NMR Chemical Shifts (δ) of Complexes **1** and **2** and the *Rac* and *Meso* Isomers of EHPG in D_2O at Various pH Values, at 298 K[a]

	EHPG (*rac*)	EHPG (*meso*)	complex **1** (*rac*)	complex **2** (*meso*)
pH*	1.38	1.33	1.37	3.41
α-H	5.08(s)	5.11(s)	4.86(s)	4.94(s), 4.81(s)[d]
methylene	3.43(m), 3.21(m)	3.33(m)	3.01(d), 2.66(d)	3.55(t), 3.32(d), 2.90(d), 2.65(t)
phenol H3[b] [H3′][c]	6.96(d)	6.98(d)	6.73(d)	6.66(d), [6.93(d)]
H4 [H4′]	7.41(t)	7.43(t)	7.40(t)	7.36(t), [7.34(t)]
H5 [H5′]	7.00(t)	7.02(t)	7.08(t)	7.02(t), [6.99(t)]
H6 [H6′]	7.28(d)	7.27(d)	7.40(d)	7.39(d), [7.34(d)]

[a] For atom labels see Chart 1. [b] Closed phenolate ring. [c] Uncoordinated phenol. [d] At 308 K.

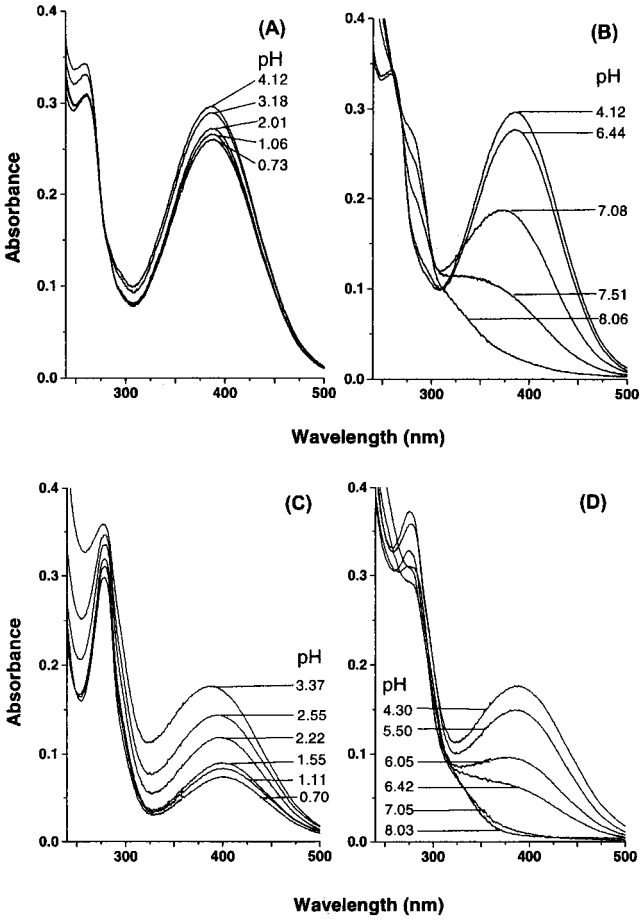

Figure 3. UV−vis spectra of complexes **1** and **2** showing the LMCT bands at various pH values: (A) complex **1**, pH 0.73−4.12; (B) complex **1**, pH 4.12−8.06; (C) complex **2**, pH 0.70−3.37; (D) complex **2**, pH 4.30−8.03. Concentration: **1**, 3.08×10^{-5} M, $\epsilon_{386} = 9600$ M^{-1} cm^{-1}, pH 4.1; **2**, 1.86×10^{-5} M, $\epsilon_{388} = 9480$ M^{-1} cm^{-1}, pH 4.3 (298 K, $\mu = 0.1$ M, 0.1 M NaCl).

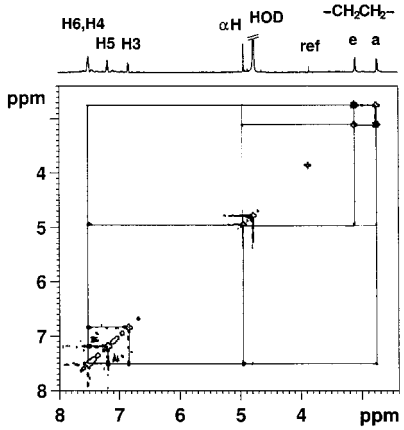

Figure 4. 2D NOESY spectrum (800 ms mixing time, 308 K) of the monomer complex **1** in D_2O (together with a COSY spectrum, Figure S3), which establishes the NMR resonance assignments. Strong NOE peaks are observed for the phenyl protons, NCH_2CH_2N protons, α-H to NCH_2CH_2N, and α-H to H6. For the labeling system, see Chart 1. **a**, axial protons; **e**, equatorial protons.

are shown in Table 3, together with data for the *meso* and *rac* isomers of the EHPG ligand. Both upfield (low-frequency) and downfield (high-frequency) shifted signals were observed for the complexes compared with the corresponding ligands. The phenolate−Ti^{IV} coordination causes a marked upfield shift of the H3 resonance (ca. 0.2 ppm for the *rac* isomer and 0.3 ppm for the *meso* isomer), but downfield shifts for H6 (ca. 0.17 ppm for *rac* and 0.10 ppm for *meso*), whereas H5 and H4 peaks are only slightly shifted (<0.08 ppm). Resonances for the uncoordinated phenol ring in the dimer complex **2** were assigned with the aid of 2D DQFCOSY and 2D NOESY NMR data. The α-H-atoms of monomeric complex **1** gave rise to a peak at 4.86 ppm, which was not affected by pH over the range 1.0−7.0, in contrast to the large chemical shift changes of the α-H-atoms of the free ligands. As expected, only one single peak was observed for the monomer **1**, indicating that the two α-H-atoms are magnetically equivalent. The ethylenediamine protons for the monomer gave rise to two deceptive quasi-quartets at 3.01 and 2.66 ppm representing an A_2B_2 system. This indicates a *gauche* conformation of the ethylenediamine portion of the EHPG ligand, similar to that observed in the solid state. The resonances for the axial protons are 0.45 ppm to higher field than those for the equatorial protons, perhaps due to differences in magnetic shielding by the phenyl rings and the diamagnetic anisotropic C−N bonds. For the dimer **2**, two single peaks (one for each of the α-H-atoms connected to the unbound phenolate and the bound phenolate) were expected for the four α-H-atoms. However, we observed only one α-H peak (2H) at 4.94 ppm at 298 K. The other peak is under the water signal at this temperature. Upon raising the temperature to >308 K, the other α-H peak (2H, 4.81 ppm at 308 K) was readily observed. 2D NOESY NMR experiments revealed connectivities between the α-H at 4.94 ppm and the bound phenolate. The ethylenediamine region of the spectrum of the dimer showed two triplets at 3.55 and 2.65 ppm, and two doublets at 3.32 and 2.90 ppm, each of which is further split into fine doublets, representing an AA′BB′ system. This indicates that the $HNCH_2CH_2NH$ groups are also fixed in a *gauche* conformation in solution. The assignment of the NMR peaks is shown in Figure 5. The chemical shifts of complexes **1** and **2** were unchanged over the pH* ranges studied (7.5−1.0 and 6.0−1.4, respectively).

pH Stability of Complexes 1 and 2. The stability of complexes **1** and **2** at different pH values was further investigated by ^{1}H NMR. Complex **1** is stable over the pH* range 1.0−7.0, but below pH* 1.0, dissociation occurred slowly, the ^{1}H NMR spectrum being consistent with the appearance of the free ligand. However, at pH* ≥ 7.5, many new peaks appeared,

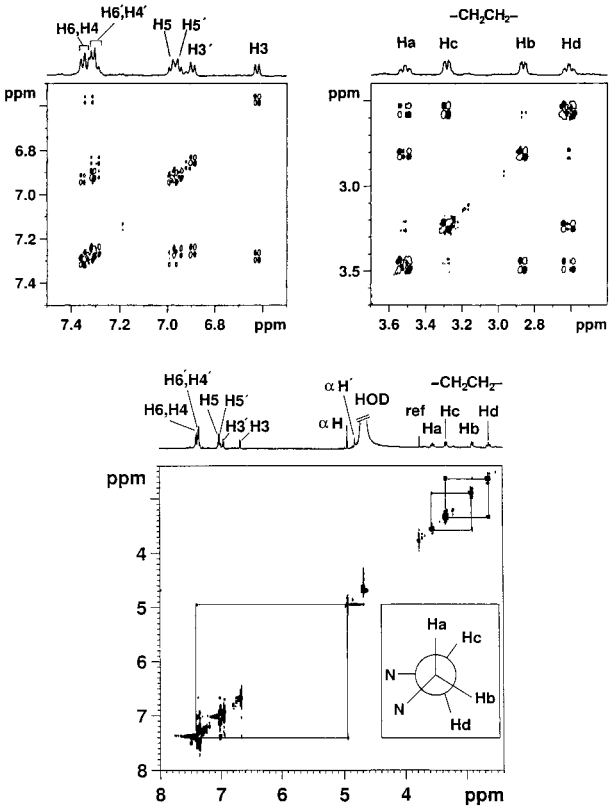

Figure 5. (A, top) 2D DQFCOSY ^{1}H NMR spectrum (500 MHz, 298 K) and (B, bottom) 2D NOESY spectrum (500 ms mixing time, 308 K) of the dimer complex **2** in D_2O, establishing the NMR resonance assignments. Strong NOE peaks are observed for the phenyl protons, for the geminal NCH_2CH_2N protons (a/b and c/d, see the inset), and for α-H to H6 for the ring-closed but not for the ring-opened side of the ligand. For the labeling system, see Chart 1.

indicating that **1** decomposes at alkaline pH (Figure S5A in the Supporting Information). Complex **2** is less stable than **1**, and only over the pH range 2.5−5.5. At pH* > 5.5, many new ^{1}H NMR resonances appeared (Figure S5B in the Supporting Information), indicating the decomposition of complex **2**. No attempt was made to identify all the decomposition products.

Reactions in Solution. The interaction between Cp_2TiCl_2 and EHPG was followed by ^{1}H NMR in D_2O at two pH* values, pH* 7.0 and 3.7. At pH* 7.0, the Cp ligands were readily released as can be seen from the decrease in intensity of the ^{1}H NMR peak for Ti^{IV}-bound Cp at 6.42 ppm, and the appearance of peaks at 6.64 and 6.57 ppm assignable to free cyclopentadiene (Figure 6).[11a] Both of the isomers of EHPG bind to Ti^{IV}, but the *rac* ligand binds faster than the *meso* isomer as can be seen from the rate of decrease of the α-H NMR peaks. The increase in intensity of the two deceptive quasi-quartets at 2.99 and 2.64 ppm (NCH_2CH_2N), the doublet at 6.72 ppm (H3), the triplet at 7.06 ppm (H5), and the multiplet at 7.39 ppm (H4 and H6) is indicative of the gradual formation of the *rac* complex **1** with a $t_{1/2}$ of ca. 50 min. However, no NMR peaks characteristic of the *meso* complex **2** were observed during the reaction, suggesting that species containing the *meso* ligand were other than complex **2** at this pH value.

At pH* 3.7, Cp_2TiCl_2 reacted very slowly with both of the EHPG isomers, as can be seen from the NMR spectra (Figure S6 in the Supporting Information). The reaction leading to the formation of the *rac* complex **1** required about one week for completion ($t_{1/2}$ of ca. 2.5 d), and weak NMR peaks characteristic of the *meso* dimer, complex **2**, did not appear until 7 d later. Deep orange crystals were isolated from the solution after 8 d at ambient temperature.

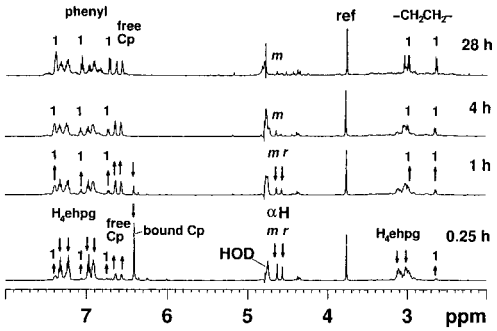

Figure 6. Kinetics of the reactions between Cp_2TiCl_2(aq) and EHPG in D_2O at pH* 7.0 and 298 K followed by ^{1}H NMR, showing the gradual release of the Cp ligands and formation of complex **1**. Peak labels: Cp, cyclopentadiene; *m* and *r*, *meso* and *rac* forms of the free ligand H_4ehpg. The same reaction at pH* 3.7 gives rise to both complex **1** and complex **2**; see Figure S4.

Discussion

The yield of monomeric complex $[Ti(ehpg)(H_2O)]\cdot(11/3)H_2O$ (**1**) or dimeric complex $[\{Ti(Hehpg)(H_2O)\}_2O]\cdot13H_2O$ (**2**) depends on pH, concentrations, and the reaction time. Complex **1** has higher solubility in water (ca. 5 mM) than complex **2** (<1 mM) and can tolerate low pH conditions. Hence, a good yield of complex **1** was achieved by reacting high concentrations (ca. 50 mM) of reactants at close to boiling temperature for 0.5 h and a pH of ca. 1.7. Crystals of **1** then formed after the solution was allowed to stand overnight at ambient temperature. Crude crystals obtained under these conditions sometimes contained trace amounts of dimer crystals of **2**, but these were readily removed by washing with cold water during filtration. Pure crystals of **1** were also obtained from reactions at higher pH (ca. 6.1) using Cp_2TiCl_2 or titanium(IV) citrate as starting material, but the yields were quite low. Complex **2** is stable only in the pH range of ca. 2.5−5.5. It is less soluble (<1 mM) in acidic solutions, but it readily dissolves at neutral pH, forming a colorless solution, which implies that **2** decomposes at neutral pH. The reaction leading to crystals of **2** is quite slow. A good yield of product was achieved after a week of reaction at ambient temperature using low concentrations (ca. 5 mM) and pH 3.7. This gave only dimer **2** without contamination by any crystals of the monomer **1**. Pure crystals of **2** were also obtained at pH ca. 1.9 or 5.0 using the same concentrations of reactants but with very low yields.

Both complexes **1** and **2** exhibit strong visible absorption bands near 387 nm. The visible bands for Fe^{III}−EHPG and VO−EHPG have been recognized as L → M charge-transfer bands involving a pπ orbital on the phenolate oxygen and half-filled d orbitals of iron or empty d orbitals of vanadium (V), respectively.[23,32] Similar bands have also been observed for other phenoxo−Ti^{IV} complexes, and assigned to ligand-to-metal charge-transfer transitions.[38] The visible bands for **1** and **2** can therefore be attributed to L → M charge transfer from a pπ orbital of the phenolate oxygen to an empty titanium d orbital. We have observed a similar broad band at 300−400 nm for Ti^{IV}−transferrin.[22,45] The CT band of the *meso* isomer is slightly red-shifted compared with that of the *rac* isomer, as is also the case for Fe^{III}−EHPG complexes.

The NMR spectra of the ligands at acidic pH have not been reported previously, probably because of the poor solubility of

(38) Harrod, J. F.; Taylor, K. R. *Inorg. Chem.* **1975**, *14*, 1541−1545.

Table 4. Comparison of Data for Metal−EHPG Complexes

metal (M)	d^n	radius[a]	CN	geom[b]	M−O[c]	M−N[c]	∠NMN[d]	∠OMO [e]	ligand	complex chirality	ref
Ti^{IV} (**2**)	0	0.68	7	pent	1.991	2.237	73.00	143.54	*meso*	N(*R*,*R*)C(*R*,*S*) or N(*S*,*S*)C(*S*,*R*)	this work
Ti^{IV} (**1b**)	0	0.68	7	pent	1.987	2.214	72.41	145.92	*rac*	N(*R*,*R*)C(*R*,*R*) or N(*S*,*S*)C(*S*,*S*)	this work
Ti^{IV} (**1a**)	0	0.68	7	pent	1.990	2.210	71.91	146.24	*rac*	N(*R*,*R*)C(*R*,*R*) or N(*S*,*S*)C(*S*,*S*)	this work
V^{IV}	1	0.63	6	oct	1.894	2.208	78.20	103.24	*rac*	N(*R*,*R*)C(*S*,*S*) or N(*S*,*S*)C(*R*,*R*)	39
Fe^{III}	5(hs)	0.64	6	oct	1.977	2.166	79.86	105.51	*rac*	N(*R*,*R*)C(*S*,*S*) or N(*S*,*S*)C(*R*,*R*)	43
Fe^{III}	5(hs)	0.64	6	oct	1.967	2.151	80.61	107.17	*rac*	N(*R*,*R*)C(*S*,*S*) or N(*S*,*S*)C(*R*,*R*)	43
Fe^{III}	5(hs)	0.64	6	oct	1.967	2.157	79.17	112.66	*meso*	N(*R*,*R*)C(*R*,*S*) or N(*S*,*S*)C(*S*,*R*)	43
Ga^{III}	10	0.62	6	oct	1.949	2.090	82.96	96.53	*rac*	N(*R*,*R*)C(*S*,*S*) or N(*S*,*S*)C(*R*,*R*)	28
Cu^{II}	9	0.72	6	oct	2.187	2.005	85.94	91.55	*rac*	N(*R*,*R*)C(*S*,*S*) or N(*S*,*S*)C(*R*,*R*)	28
Co^{III}	6(ls)	0.63	6	oct	1.907	1.938	86.59	87.14	*rac*	N(*R*,*R*)C(*S*,*S*) or N(*S*,*S*)C(*R*,*R*)	28

[a] Ionic radius (Å). [b] Key: pent, pentagonal bipyramid; oct, octahedral. [c] Average bond distance (Å). [d] NMN angle (deg). [e] The OMO angle *trans* to the NMN angle (deg).

the ligand at low pH values.[32,33] However, the commercial EHPG ligand readily dissolves in D_2O at pH* values below 2, which may be due to the protonation of the carboxylate groups of the ligand. Resonances for all the protons of the *rac* and *meso* isomers of EHPG were well resolved and have been unambiguously assigned for the first time in this work.

The Ti^{IV} complexes of both the *rac*- and *meso*-EHPG ligand are seven-coordinate with a water molecule as a coligand (Figure S7 in the Supporting Information). In the crystal structure of **2**, one of the phenol groups of the Hehpg ligand is not coordinated, and is present in the ring-opened form. The only reported ring-opened metallo-EHPG complex[39] is the octahedral vanadyl complex [VO(Hehpg)], containing one ring-opened phenol. Similar to **2**, the vanadyl complex is stable only under weakly acidic conditions. In transferrin, Fe^{III} is coordinated to two deprotonated phenolates (Tyr residues), but intermediates with just one bound Tyr may be formed during metal uptake and release. The detection of ring-opened model complexes is therefore of significance.

Ti^{IV} has empty 3d orbitals and an ionic radius of ca. 0.68 Å.[40] Similar to its $4d^0$ and $5d^0$ analogues Zr^{IV} and Hf^{IV},[40] Ti^{IV} is readily isolated in solvated form, with the metal achieving seven-coordination. Several X-ray structures of seven-coordinate complexes have been reported.[37a,40,41] It has been suggested[37a] that a spherically symmetric charge distribution favors pentagonal-bipyramidal geometry if the central metal ion is of sufficient size to tolerate a coordination number higher than 6, or if the ligand-field splitting does not greatly favor an octahedral arrangement. With its relatively large size, and a spherically symmetric charge distribution, Ti^{IV} can adopt coordination numbers from 2 to 11. Our examination of a number of X-ray crystal structures in the Cambridge Structure Database (ca. 1000) suggested that the most common coordination number is 4 (ca. 45%), followed by 6 (ca. 18%) and 5 (ca. 16%), with about 2.5% having a coordination number of 7.

Hoard et al. have pointed out[42] that, for metal−EDTA complexes, as the size of the central ion increases and the M−N bond lengths increase, seven-coordination becomes favorable via the binding of a water molecule to fill the "hole" created by expansion of O−M−O bond angles *trans* to M−N bonds. This seems to be the case for metal−EHPG complexes. Table 4 compares data for available X-ray crystal structures of metal−EHPG complexes. It can be seen that Ti^{IV} has a relatively large ionic radius (0.68 Å), and that Ti^{IV}−EHPG complexes have the longest M−N bonds (>2.2 Å), and therefore the smallest N−M−N angles. Modeling studies reveal that increases in the M−N bond lengths lead to movement of the *trans* oxygen atoms connected to the nitrogens by chelate rings and to concomitant opening of the corresponding O−M−O bond angles *trans* to the M−N bonds. In the case of Ti^{IV}−EHPG complexes, the M−N bond lengths are long and the N−M−N angles are small (71−73°). Concomitant opening of the O−M−O bond angles *trans* to the M−N bonds is large enough (>143.5°) to encourage the coordination of a water molecule in the large hole thus formed. Therefore, it is understandable that Ti^{IV} becomes seven-coordinate in these circumstances. The V^{IV}−EHPG complex also has long V−N bonds, but V(IV) has a smaller ionic radius (0.63 Å), one of the oxygen ligands (V=O) in the *trans* O−V−O unit is not connected by a chelate ring (one of the phenolates is not coordinated to V^{IV} in this complex), and the O−V−O angle is only 103°, not large enough to accommodate a water molecule.

A similar analysis may also apply to the spherically symmetric high-spin d^5 Fe^{III}−EHPG complexes, which also have relatively long Fe−N bond lengths (ca. 2.16 Å) and a medium ionic radius for Fe^{III} (0.64 Å). Although they are six-coordinate in the crystal lattice with O−Fe−O angles of 105−112°, optical spectroscopic properties suggest that Fe^{III}−EHPG may be seven-coordinate in aqueous solution with an additional bound water ligand.[29]

The most distinguishing feature of these Ti^{IV}−EHPG structures is their stereochemistry. The EHPG ligand itself contains two chiral carbon atoms, so it has two diastereomeric forms, a pair of enantiomers (*R*,*R* and *S*,*S*) and a *meso* form (*R*,*S* or *S*,*R*). However, the EHPG ligand contains two prochiral nitrogen atoms, and so the two amine nitrogens become chiral when bound to a metal. Thus, there are four chiral atoms in metal−EHPG complexes, resulting in a total of 16 possible configurations. As discussed earlier,[34] only a *gauche* conformation for the NCH_2CH_2N group in the metal complexes is possible. This constraint and the 2-fold axis in the *meso* conformers reduce the original 16 possible conformers to only 6.

In the three conformers with nitrogen atoms in the N(*S*,*S*) configuration, the chiral carbon atoms can be labeled as C(*R*,*R*), C(*S*,*S*), and C(*R*,*S*). If the nitrogen atoms are in the N(*R*,*R*) form, a similar argument holds, since they are mirror images of the three N(*S*,*S*) conformers. The complex with absolute chirality of N(*S*,*S*)C(*R*,*R*), which has been designated as (*R*,*R*) *rac*[34] or Λ*RR*[28] in some previous reports, and its mirror image isomer N(*R*,*R*)C(*S*,*S*), Δ*SS*,[28] have the six-membered phenolate chelate rings in the equatorial positions and five-membered carboxylate chelate rings in axial sites. One of the mirror isomers with the

(39) Riley, P. E.; Pecoraro, V. L.; Carrano, C. J.; Bonadies, J. A.; Raymond, K. N. *Inorg. Chem.* **1986**, *25*, 154−160.
(40) (a) Mazzanti, M,; Rosset, J.-M.; Floriani, C.; Chiesi-Villa, A.; Guastini, C. *J. Chem. Soc., Dalton Trans.* **1990**, 1335−1344. (b) Corazza, F.; Solari, E.; Floriani, C.; Chiesi-Villa, A.; Guastini, C. *J. Chem. Soc., Dalton Trans.* **1990**, 1335−1344.
(41) Coles, S. J.; Hursthouse, M. B.; Kelly, D. G.; Toner, A. J.; Walker, N. M. *J. Chem. Soc., Dalton Trans.* **1998**, 3489−3494.
(42) Stezowski, J. J.; Countryman, R.; Hoard, J. *Inorg. Chem.* **1973**, *12*, 1749−1754.

Chart 2. Schematic Drawing of Octahedral M−EHPG Isomers[a]

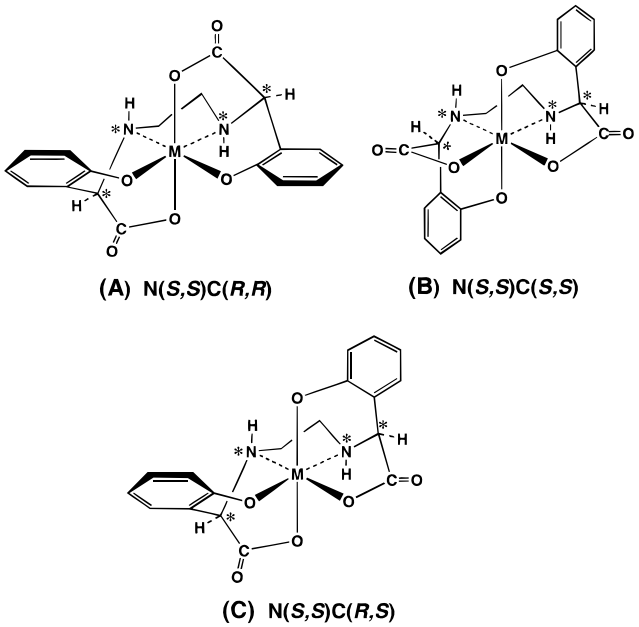

[a] The asterisks indicate chiral atoms.

N(*S*,*S*)C(*R*,*R*) configuration is shown in Chart 2A. The complex with N(*S*,*S*)C(*S*,*S*), which has been designated as (*S*,*S*) *rac*[34] or Δ*RR*,[28] in the literature, and its mirror isomer N(*R*,*R*)C(*R*,*R*) both have the six-membered chelate phenolate rings in axial sites. One of the mirror isomers with the N(*S*,*S*)C(*S*,*S*) configuration is shown in Chart 2B. The N(*S*,*S*)C(*R*,*S*) *meso* isomer, which has been designated as (*R*,*S*) *meso* in the literature, and its mirror isomer N(*R*,*R*)C(*S*,*R*) have one axial and one equatorial phenolate, as shown in Chart 2C.

Although X-ray crystal structures containing the N(*S*,*S*)C(*R*,*R*) and N(*R*,*R*)C(*S*,*S*) ((*R*,*R*) *rac*, Λ*RR* and Δ*SS*) conformers of Fe^{III}, Co^{III}, Ga^{III}, Cu^{II}, and V^{IV} and the (*R*,*S*) *meso* conformer of Fe^{III} are available, the crystal structure of a complex containing the corresponding N(*S*,*S*)C(*S*,*S*) or N(*R*,*R*)C(*R*,*R*) ((*S*,*S*) *rac*, Λ*SS* or Δ*RR*) conformer has not yet been reported, as far as we are aware. The absence of the N(*S*,*S*)C(*S*,*S*) or N(*R*,*R*)C(*R*,*R*) ((*S*,*S*) *rac*, Λ*SS* or Δ*RR*) conformers in crystals has previously been ascribed to unfavorable crystal packing,[43] or to the inherent instability of the *(S,S) rac* conformer.[28] Molecular mechanics studies[34] of Fe^{III}−EHPG complexes show that the most stable conformers are the N(*S*,*S*)C(*R*,*R*) and N(*R*,*R*)C(*S*,*S*) ((*R*,*R*) *rac*, Λ*RR* and Δ*SS*), both in vacuo and in aqueous solution, while the least stable is the N(*S*,*S*)C(*S*,*S*) or N(*R*,*R*)C(*R*,*R*) ((*S*,*S*) *rac*, Λ*SS* or Δ*RR*) conformer. Stability constants for the *(R,R) rac* and *(R,S) meso* complexes of EHPG with a few metal ions (Fe^{III}, Ni^{II}, Zn^{II}, Cu^{II}, Ga^{III}, and In^{III}) have been determined,[33] and the results show that all the *(R,R) rac* conformers are more stable by 2−3 kcal/mol than the *(R,S) meso* conformer for all the metal ions studied. Thus, the presence of the *(S,S) rac* conformers (N(*S*,*S*)C(*S*,*S*) and its mirror isomer N(*R*,*R*)C(*R*,*R*) as pairs in the unit cell) in crystals of **1** was unexpected. In crystals of the dimer **2**, both Ti^{IV}−EHPG units are in the *(R,S) meso* form (N(*R*,*R*)C(*R*,*S*) for both EHPG ligands with its mirror isomer N(*S*,*S*)C(*S*,*R*) also present in the unit cell). None of the preparations gave rise to Ti^{IV}−EHPG N(*S*,*S*)C(*R*,*R*) or N(*R*,*R*)C(*S*,*S*) ((*R*,*R*) *rac*, Λ*RR* and Δ*SS*) isomers, which have always been observed for other metals studied so far.

For octahedral metal−EHPG complexes, greater stability has been proposed[33,34] for *(R,R) rac* isomers due to the geometric selectivity in the placement of both six-membered chelate rings in the equatorial plane defined by the ethylenediamine ring. In the *(S,S) rac* conformer, both of the six-membered chelate rings are in the axial position, which is a very strained arrangement. In the case of the *(R,S) meso* isomer, the only possible arrangement is the one with all coordinating groups *cis* to one another, that is, one axial phenyl and one equatorial phenyl. This structure is intermediate between the highly strained *(S,S) rac* arrangement and the most favorable *(R,R) rac* arrangement.

The unusual N(*S*,*S*)C(*S*,*S*) or N(*R*,*R*)C(*R*,*R*) ((*S*,*S*) *rac*, Λ*SS* or Δ*RR*) chirality of Ti^{IV}−EHPG in **1** can be understood by considering the factors leading to metal complex stability. The two major factors are ligand basicity and coordination geometry.[33] Experimental results have suggested that the two isomers of EHPG have the same basicities (*rac* 38.0 and *meso* 37.9).[33] Therefore, the coordination geometry is likely to play a major role. Since the bite angle of a six-membered chelate ring[28,44] is about 90−95° and substantially greater than that of a five-membered chelate ring (ca. 70−80°),[28,44] more satisfactory octahedral coordination is achieved with both six-membered rings bound to the metal in the equatorial plane that contains the five-membered ethylenediamine group. This is the case for the *(R,R) rac* conformation in most of the reported metal−EHPG complexes. For the Ti−EHPG complexes, Ti^{IV} is seven-coordinate with pentagonal-bipyrimidal geometry, which will be very strained if any of the six-membered chelate rings bound to the metal are in the pentagonal plane. More satisfactory pentagonal-bipyrimidal coordination is achieved with the six-membered chelate rings in the axial position, which results in the ring-closed monomer [Ti(ehpg)(H_2O)]·(11/3)H_2O (**1**) crystallizing as the N(*S*,*S*)C(*S*,*S*) and N(*R*,*R*)C(*R*,*R*) ((*S*,*S*) *rac*, Λ*SS* or Δ*RR*) isomers, and the (*R*,*S*) *meso* ligands forming the ring-opened oxo-bridged dimer [{Ti(Hehpg)(H_2O)}$_2$O]·13H_2O (**2**).

Titanium(IV) readily forms complexes with EHPG(*rac*), a chelating amino acid derivative, at neutral pH. This has implications for the mechanism of action of titanium anticancer drugs. Ti^{IV} is very "hard" and readily hydrolyzes to form insoluble polymeric species at neutral pH. Both titanocene dichloride and Budotitane undergo rapid and complete hydrolysis to form insoluble polymers at physiological pH.[2,11a] However, biological experiments reveal that titanium is accumulated in the cellular nucleic-acid-rich regions (mainly the nucleus) after in vivo application of titanium drugs.[7] Therefore, biomolecules must be involved in the stabilization of Ti^{IV} and its transport. The present work shows that Ti^{IV} can bind to EHPG(*rac*) at neutral pH, and is thought to bind in a manner similar to that of to transferrin.[22,45] Both titanium (IV) citrate and Cp_2TiCl_2-(aq) can transfer Ti^{IV} to the specific Fe^{III} sites of human apotransferrin at pH 7.4. Transferrin may therefore serve to deliver Ti^{IV} from the antitumor drug Cp_2TiCl_2 or Budotitane to cancer cells, which are known to have a higher density of transferrin receptors than normal cells,[46] and may release the metal in endosomes inside cells. This may allow these drugs to target biomolecules such as nucleic acids at low pH, or subsequently to bind to other phenolate proteins. Either of these

(43) (a) Bailey, N. A.; Cummins, D.; Mckenzie, E. D.; Worthington, J. M. *Inorg. Chim. Acta* **1976**, *18*, L13. (b) Bailey, N. A.; Cummins, D.; Mckenzie, E. D.; Worthington, J. M. *Inorg. Chim. Acta* **1981**, *50*, 511.
(44) Bannochie, C. J.; Martel, A. E. *Inorg. Chem.* **1991**, *30*, 1385−1392.
(45) Guo, M.; Sun, H.; Sadler, P. J. Manuscript in preparation.
(46) Wagner, E.; Curiel, D.; Cotten, M. *Adv. Drug. Delivery Rev.* **1994**, *14*, 113.

routes could result in Ti^{IV} inhibition of DNA synthesis and mitotic activity. Recently, Marks and co-workers also suggested that enzymes could also be targets for metallocene anticancer drugs.[10a] Further biological investigations of titanium transferrin or other phenolate proteins are therefore warranted.

Acknowledgment. We thank the Committee of Vice-Chancellors and Principals for an ORS award, the University of Edinburgh for a scholarship (M.G.), and the EPSRC (studentship for S.B.) and BBSRC for support. We are grateful to Dr X. Tan (Edinburgh) for his kind advice on crystallization.

Supporting Information Available: Figure S1 [molecular structure and atom-labeling scheme for one of the mirror isomers of complex **1b**], Figure S2 [500 MHz ^{1}H NMR spectra of commercial EHPG and its *rac* and *meso* isomers at acidic pH* values in D_2O], Figure S3 [500 MHz [^{1}H,^{1}H] (A) COSY and (B) NOESY (mixing time 1.2 s) spectra of the EHPG(*rac*) isomer in D_2O at 310 K, which establish the NMR resonance assignments], Figure S4 **[**2D [^{1}H,^{1}H] COSY ^{1}H NMR spectrum (500 MHz, 298 K) of the monomer complex **1** in D_2O], Figure S5 [^{1}H NMR spectra of (A) complex **1** and (B) complex **2** at different pH^* values], Figure S6 [kinetics of the reactions between Cp_2TiCl_2-(aq) and EHPG in D_2O at pH* 3.7 followed by ^{1}H NMR], and Figure S7 [a color picture showing the intramolecular hydrogen bonds in complexes **1** and **2**]. This material is available free of charge via the Internet at http:/pubs.acs.org.

IC990669A